ON – LINE PARAMETER EVALUATION OF THREE PHASE INDUCTION MOTOR WITH GNA

D. K. Chaturvedi[1], Mayank Pratap Singh[2], O.P. Malik[3]

[1]Professor, Dept. of Electrical Engineering, D.E.I., Dayalbagh, Agra, U. P., INDIA
[2]Assistant Professor, Dept. of Electrical Engineering, G. L. A. University, Mathura, U. P., INDIA
[3]Emeritus Professor, Dept. of Electrical and Computer Engineering, University of Calgary, AB, Canada

---

Abstract-*The three phase induction motors (TPIMs) are very frequently encountered in industrial environment for rotating mechanical loads. TPIM behavior is totally dependent on its parameters. The TPIM parameter information tells about the health of induction motor and also necessary for precise control of its behavior.*

In this paper the GNA is used for parameter estimation of TPIM. GNA is trained offline using simulated results and then deployed for on-line parameter evaluation of squirrel cage TPIM in the Electrical Power Research Lab, D.E.I. (Deemed University) Dayalbagh, Agra. The proposed method is compared with simple neural approach, and experimentally obtained parameters.

***Keywords*—Parameter Estimation, Three Phase Induction Motor (TPIM), Artificial Neural approach (ANA), Generalized Neural Approach (GNA), Equivalent Circuit Parameters, Soft Computing Techniques.**

I. INTRODUCTION

The soft Computing Approaches has been broadly used for data analysis during abnormal situations. These approaches are further categorized as expert systems [1], Fuzzy Logic System(FLS) [2, 3], fuzzy neural approach (FNA) [4-13], wavelet transform [14-16], and genetic approach [17].

The TPIM parameters are not constant during its working and changes non-linearly. The parameters vary with weather conditions, operating temperature, magnetic, electrical and mechanical couplings, etc. Therefore, its parameters estimated from above discussed methods could not give good results [18-19].

In the area of electrical machines and power system ANA is widely used in the last 2-3 decades [20-31]. ANA can handle large size information at a time because of its parallel processing capability. Hence, it is an effective approach for TPIM parameter evaluation. Although, ANA can do non-linear mapping of input-output vary well and extrapolate the results for ill defined or noisy data, it has certain inherent shortfalls. ANA needs large number of examples for good training, large training time, no specific ANA structure and configuration for a problem in hand. The neuron structure is also not known such as summation type, or product type or combination etc.

The paper is divided in eight sections. First section deals with the introduction of the work, followed by sections two describes GNN tool. Section third to fifth deal with experimentation on TPIM. Section sixth contains online parameter estimation of TPIM and finally the section describes conclusion of the work and references.

1.1 Generalised Neural Approach (GNA)

To defeat the above mentioned problems, Generalized Neuron Approach (GNA) has been built up with the help of diverse compensatory functions at aggregation and doorstep function as activation for GNA as shown in Fig. 1. The back-propagation-training algorithm is used [32-33]. After Learning use the Generalized Neural Approach (GNA) for TPIM parameter estimation.

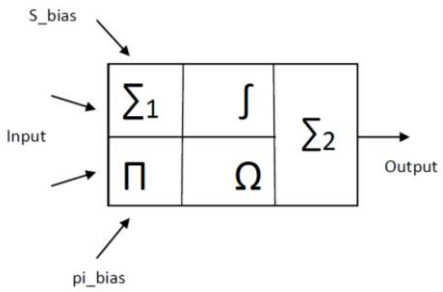

Fig-1: GNA Model

The TPIM is approximated as the transformer with the exemption that its secondary coils are liberated for angular motion. The approximated circuit of TPIM is shown in Fig.1

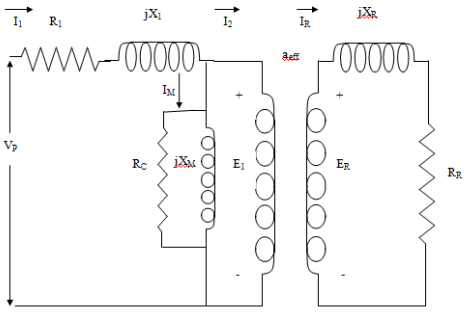

Fig.2: Approximated Circuit of TPIM

The rotor frequency of TPIM i.e.$f_r = s * f_s$

It is recognized that $X = \omega L = 2\pi fL$ means the rotor reactance is dependent of rotor frequency and changes as $X_R = s * X_{R0}$, Where X_{R0} - rotor reactance at the applied frequency (when rotor is stationary). The rotor approximated network of rotor is shown in Fig.2.

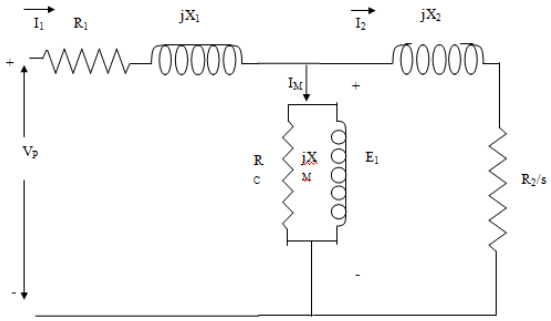

Fig-3: Approximated Network of TPIM

In this figure E_R is induced rotor network voltage and R_R is the rotor network resistance.
The rotor network current (I_R) can be calculated as given in equation.

$$I_R = \frac{E_R}{(R_R + jX_R)} = \frac{E_R}{(R_R + jsX_{Ro})}$$

The equation can be re-written as:

$$I_R = \frac{E_{R0}}{\left(\frac{R_R}{s} + jX_{R0}\right)}$$

E_{R0} is the rotor induced voltage when rotor is stationary and X_{R0} is the rotor network reactance at unity motor slip. The customized rotor approximated network can be given in Fig. 3.

Where

$$X_2 = a_{eff}^2 X_{Ro}$$

$$R_2 = a_{eff}^2 R_R$$

$$I_2 = \frac{I_R}{a_{eff}}$$

$$E_1 = a_{eff}^2 E_{Ro}$$

$$a_{eff} = \frac{N_s}{N_R}$$

II. ZERO SHAFT LOAD AND STATIONARY ROTOR TESTS FOR DETERMINATION OF TPIM APPROXIMATED CIRCUIT PARAMETERS

The delta connected TPIM is energized by balanced three phase, 415 V, 50 Hz AC supply through three phase auto-transformer. Also a voltmeter, ammeter and two wattmeters are connected to measure voltage, current and power of TPIM under different test conditions as shown in Fig. 4.

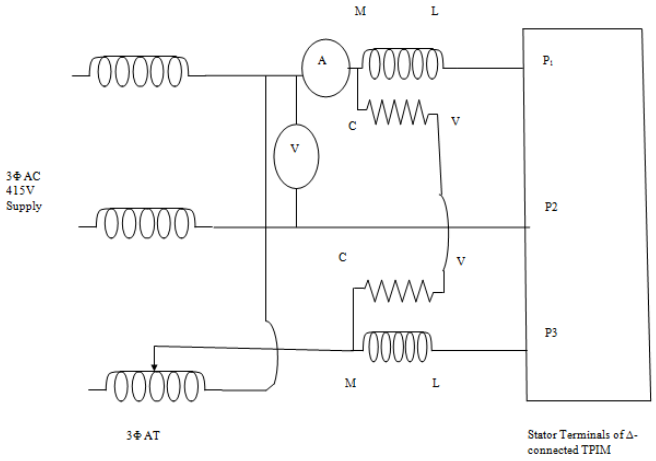

Fig-4: Circuit diagram for experimentation

1. 1. Zero Shaft Load Test

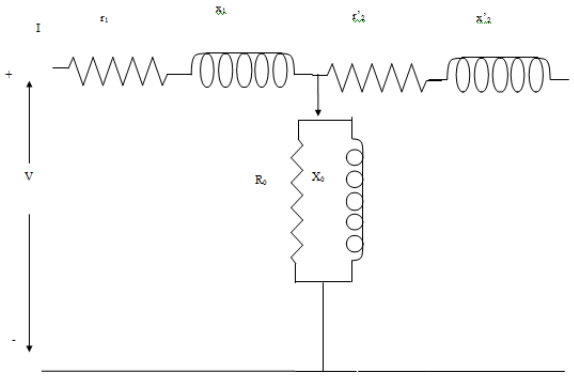

Fig-5: Approximated Circuit for Zero Shaft Load Test

Under Zero shaft load condition the rotor current is negligibly small and hence the approximated rotor circuit is open as shown in Fig. 5. The rotor of TPIM is permitted to rotate without restraint under zero shaft load condition at specified terminal voltage and supply frequency. The speed of TPIM is quite close to synchronous speed (i.e. slip nearly zero). In this situation voltage, current and power are measure. The shunt parameters can be calculated as Z_o, R_o and X_o in equation given below.

$Z_0 = \frac{V}{\left(\frac{I}{\sqrt{3}}\right)}, R_0 = \frac{P}{I^2}$ and $X_0 = \sqrt{(Z_0^2 - R_0^2)}$

Where V, I, P are called no load voltage, current and power and

Z_o- no load impedance in ohms,

R_o-no load resistance in ohms,

X_o-no load reactance in ohms.

2. Stationary Rotor Test

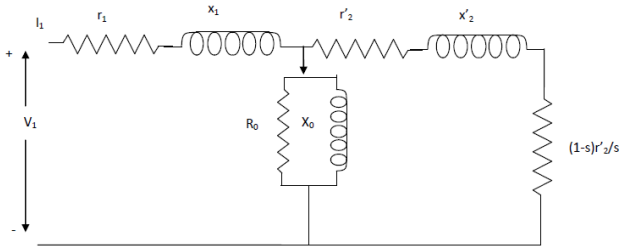

Fig-6: Approximated Circuit for Stationary Rotor Test

In stationary rotor condition, the rotor will not rotate. Hence, a small voltage applied to stator terminals of motor results huge current to flow. The Approximated circuit under stationary rotor condition is shown in Fig. 6. Therefore, connect TPIM to a controllable- AC supply and regulate the applied voltage under the stationary-rotor, till the TPIM current is equal to the nameplate current. Determine voltage, current and power. Now we determine equivalent resistance and equivalent reactance from equation given below.

$$Z_b = \frac{V_b}{\left(\frac{I}{\sqrt{3}}\right)}, R_b = \frac{P}{I_b^2} \text{ and } X_b = \sqrt{(Z_b^2 - R_b^2)}$$

Where V_b, I_b, P are called blocked rotor voltage, current and power and

Z_b-equivalent impedance in ohms,
R_b-equivalent resistance in ohms = r_1+r_2',
r_1 – Stator resistance in ohms
r_2 – Rotor resistance in ohms referred to stator side
X_b-equivalent reactance in ohms = x_1+x_2'.
x_1 – Stator reactance in ohms
x_2 – Rotor reactance in ohms referred to stator side

1. Zero Shaft Load Test at different voltages

V= [320, 340, 360, 380, 400, 420, 430, 440] Volts
I= [2.5, 2.8, 3, 3.2, 3.4, 3.7, 4, 4.2] Amps
P= [200, 220, 225, 240, 270, 290, 320, 340] Watts

2. Stationary Rotor Test at different currents

V_b= [174, 179, 184, 190, 196, 220, 225, 230] Volts
I_b= [6, 6.25, 6.5, 7, 7.35, 7.7, 7.75, 7.8] Amps
P_b= [780, 860, 940, 1100, 1200, 1220, 1300, 1400] Watts

III. EXPERIMENTAL SETUP

The tests conducted in Electrical Power Research lab at Department of Electrical Engineering, Faculty of Engineering, D.E.I. (Deemed Univ.) Agra, India. The laboratory set up for parameter evaluation of TPIM is consisting of the following components as shown in Fig. 7:
a. TPIM with outside winding connection facility
b. Sensors / Transducers (Current, Voltage, and Speed)
c. Data Acquisition system
d. Signal conditioning /processing devices
e. Suitable software / tools for Parameter Estimation

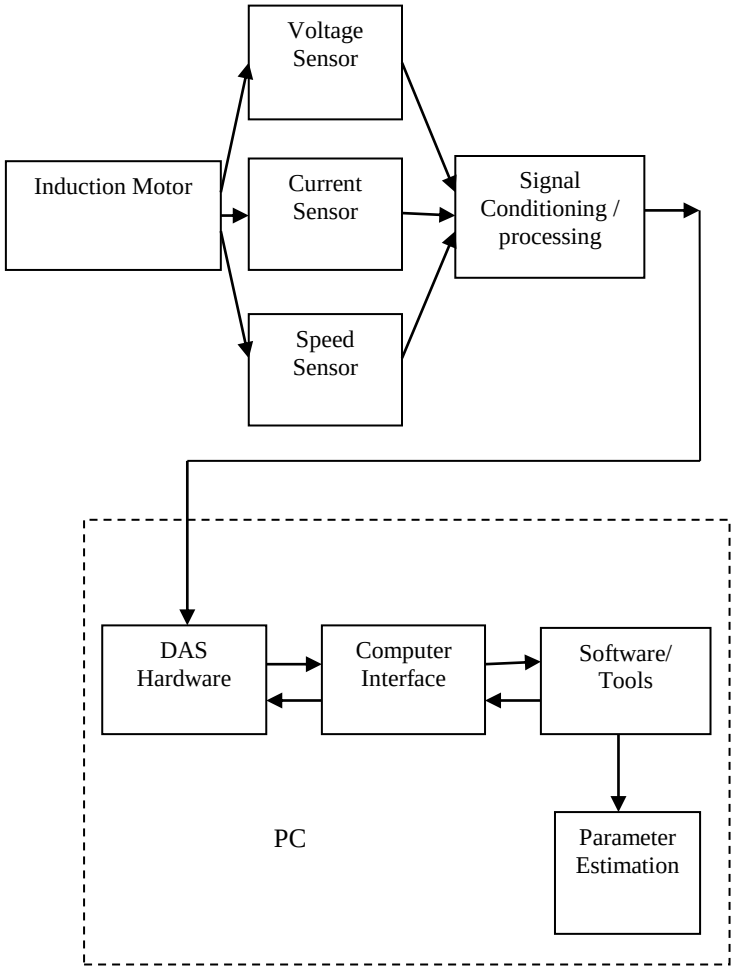

Fig-7: Block diagram Parameter Estimation System for TPIM

These components of block diagram shown in Fig. 7 are discussed in the following sections.

TPIM with outside winding connection facility

The TPIM with outside winding connection facility is shown in Fig.8. The motor stator windings are connected for four pole delta connected machine as shown in Fig. 9. The experiment setup is consisting of the 5 hp, three phase,

415V, 7.8A, 50Hz Squirrel cage TPIM. The motor specifications are given in Table – 1.

Table – 1: Specifications of TPIM

Number of poles	2,4,6,10,12 (By changing coil connections)
External dia of TPIM Stator	25.5 cm
Internal dia of TPIM Stator	12.18 cm
Gap between stator and rotor	0.325cm
Length of Si-steel core	6.25 cm
Dia of TPIM shaft	3.4 cm
Rotor slot length	1.33 cm
No. of stator slots	36
No. of rotor slots	28
specified voltage (line)	440 volts
specified frequency	50 Hz
specified power	3.75kW
Skew	0.425

Fig-8: TPIM with outside winding connection facility

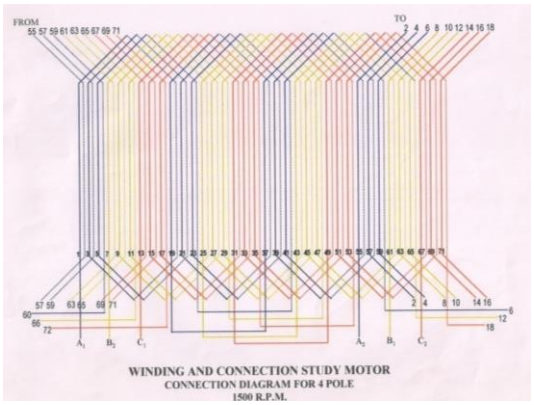

Fig-9: Stator pole diagram of 4-pole TPIM

5.3.2 Sensors / Transduceers (Current, Voltage and Speed)

For the measurement of voltage and current the sensors are developed in the lab and calibrated by voltage-current - frequency (VIF) meter. The speed transducer is developed using a coil wound on a permanent magnet and iron strips of the cooling fan passes at a close distance from magnet as shown in Fig. 10. As these iron strips pass just below the magnetic pole, the flux linkage changes which results in the voltage waveform as shown in Fig. 11-12. The LabVIEW Virtual Instrument (VI) for measurement of speed is shown in Figs. 13-14.

Data acquisition system (DAS)

Data acquisition system (DAS) contains the data acquisition hardware and suitable software. The main function of this hardware is to convert various electrical and mechanical analog signals like armature current, voltage, power, speed and vibration to digital signals through ADC and vice-versa through DAC as per the requirements. These digital signals are used by the computer to convert into useful information that a computer can read, and analyzed to extract meaningful information. The ADC is used in the DAS card for analog to digital converter. After ADC, S/H network is used to digitize and hold the signal. As the name indicates, S/H network is a network whose purpose is to digitize an input analog signal and hold its last digitized value until the input is taken. A microcontroller is used to interface the sensor output with computer. The microcontroller used in this DAQ card is MICRO –CONTROLLER ATMEGA16A PU 1339. The data acquisition system and its block diagram are shown in Figures 15 and 16.

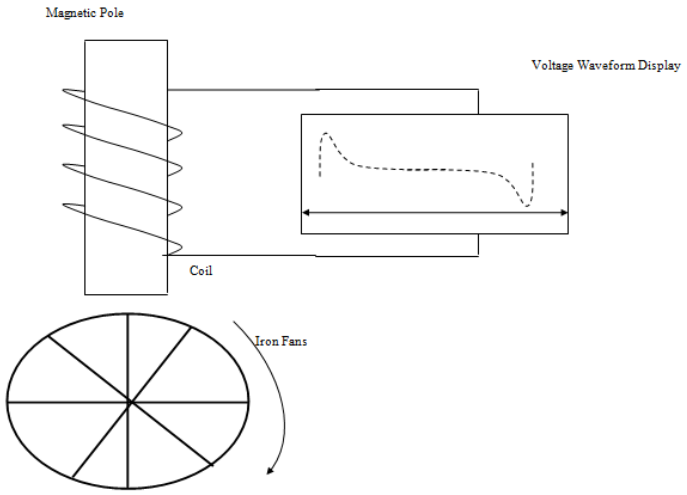

Fig-10: Coil on the magnet

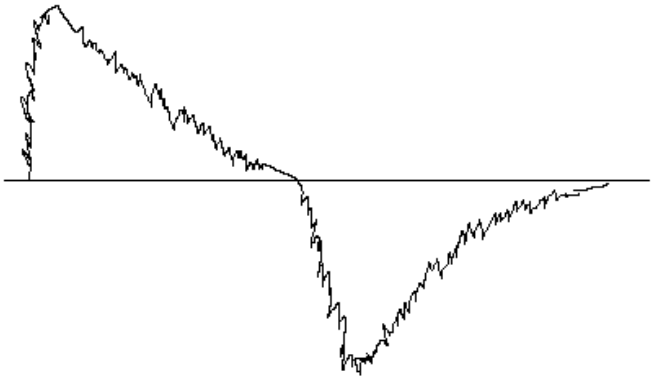

Fig-11: Induced voltage waveform with noise

Fig-12: Induced voltage waveform without noise

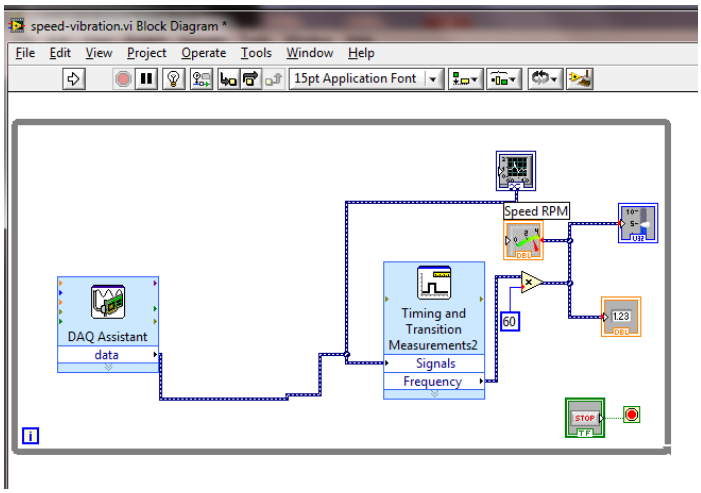

Fig-13: LabVIEW interfacing VI for Speed measurement

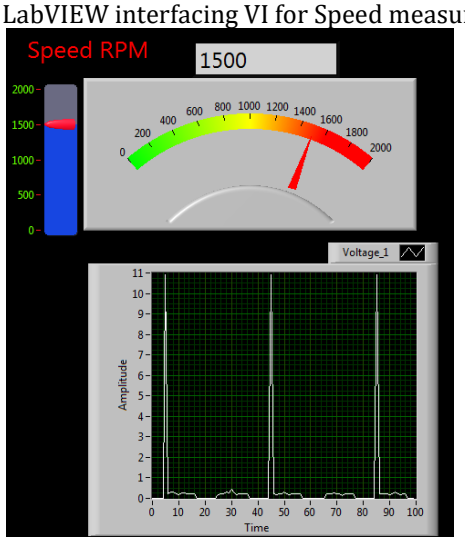

Fig- 14: Screen shot for Speed measurement at No-load

Fig-15: Data Acquisition System

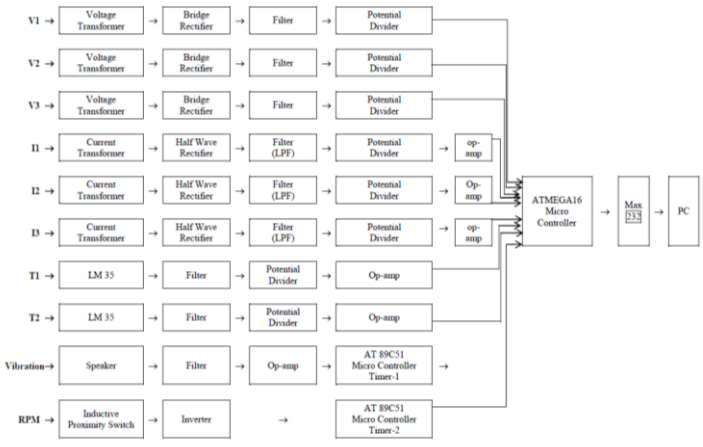

Fig-26: Block Diagram of sensors and DAQ system

This section deals with the experimentation with TPIM under different operating conditions and loads.

The experimental results of healthy TPIM under different loading conditions are as:

Fig.17 shows the applied load on the shaft of TPIM under different loading conditions when motor is healthy or windings are short circuited by 10%, 20% or 30%.

Fig. 18 shows three phase voltages of healthy TPIM under different loading conditions (no-load, light load, full load and overload). Figs. 19 shows three phase currents of healthy TPIM,

Fig. 20 shows that the speed of TPIM decreases as the load torque increases.

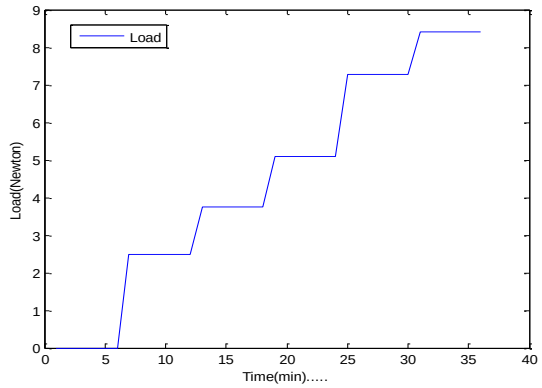

Fig-17: Load applied on TPIM under different loading conditions

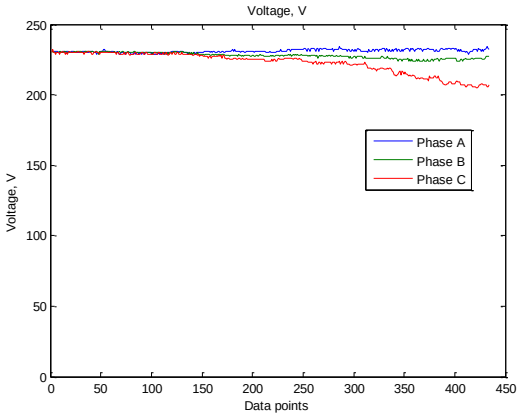

Fig-38: Phase *a, b* and *c* Voltage of Healthy TPIM under different loading conditions

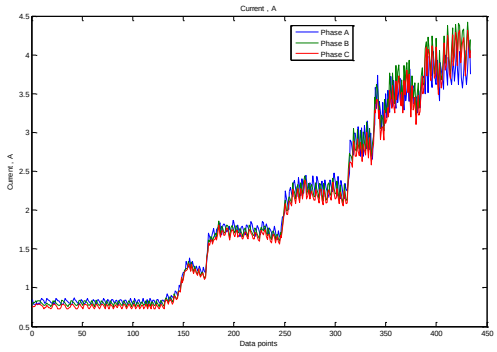

(a) When motor is healthy

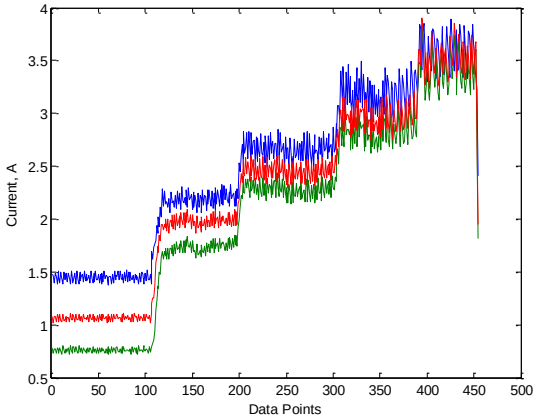

(b) When one Phase is shorted by 10% of TPIM through R=3.1 ohm

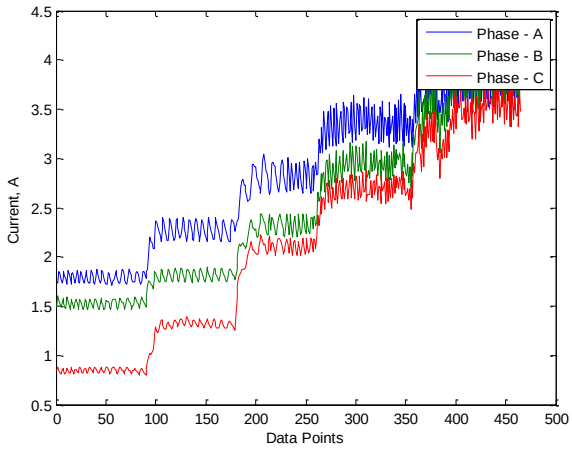

(c) When 10% of each Two Phases are short circuited of TPIM through resistance R=3.1 ohm

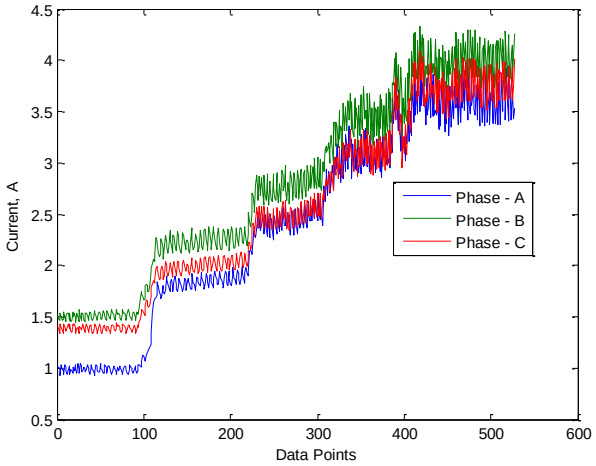

(d) When 10% of each Three Phases are short circuited of TPIM through resistance R=3.1 ohm

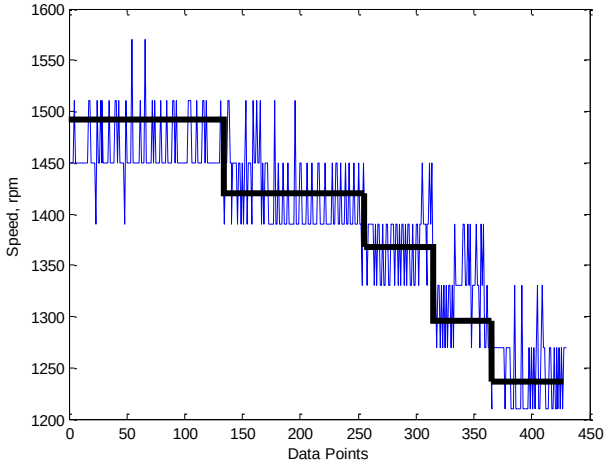

(a) Speed of Healthy TPIM

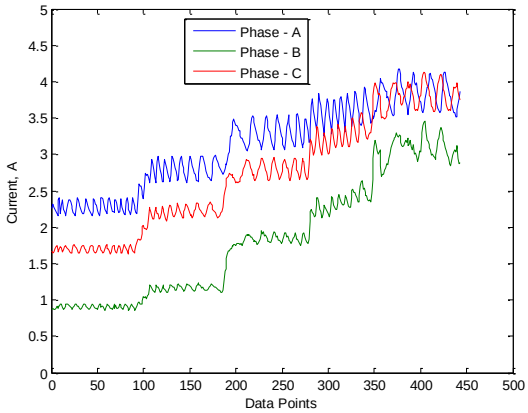

(e) When one Phase is shorted by 20% of TPIM through R=3.1 ohm

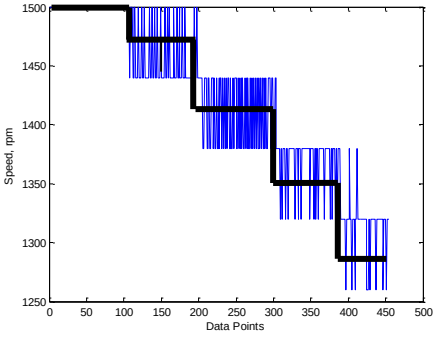

(b) When one Phase is shorted by 10% through R=3.1 ohm

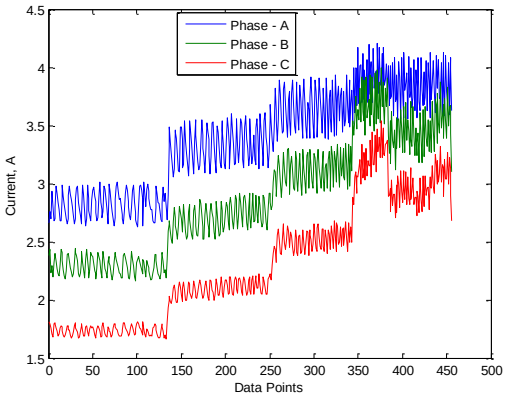

(f) When 20% of each Two Phases are short circuited of TPIM through resistance R=3.1 ohm

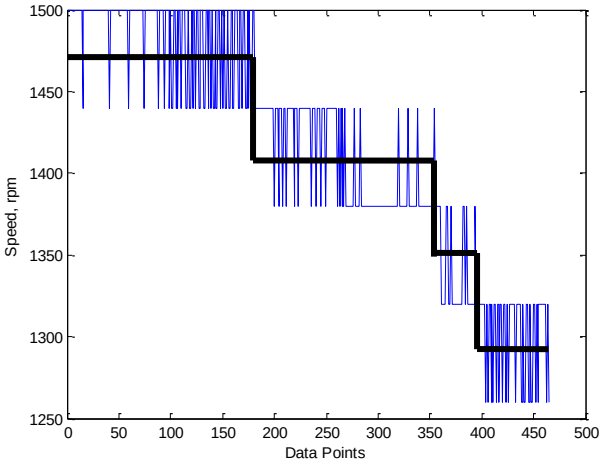

(c) When 10% of each Two Phases are short circuited through resistance R=3.1 ohm

Fig-19: Currents of Phase *a, b* and *c* of TPIM under different loading conditions

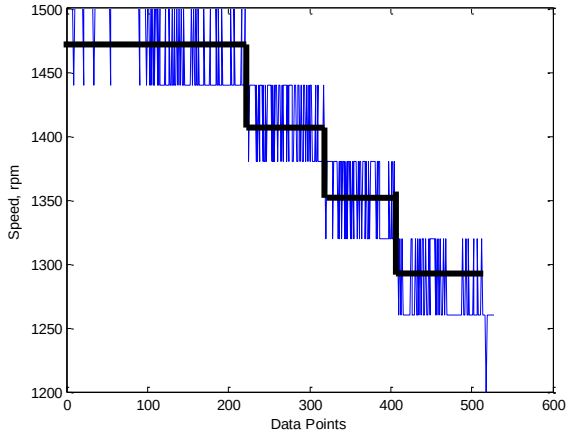

(d) When 10% of each Two Phases are short circuited through resistance R=3.1 ohm

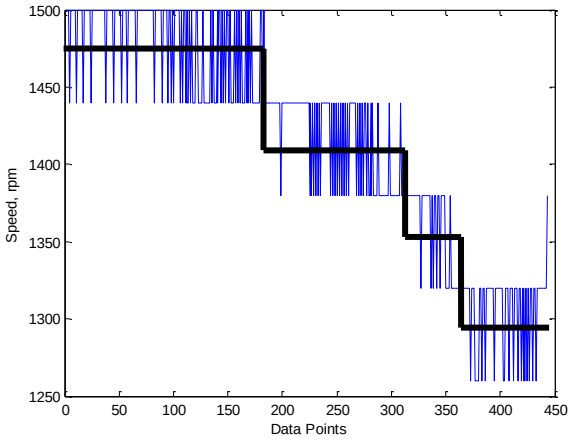

(e) When one Phase is shorted by 20% through R=3.1 ohm

0

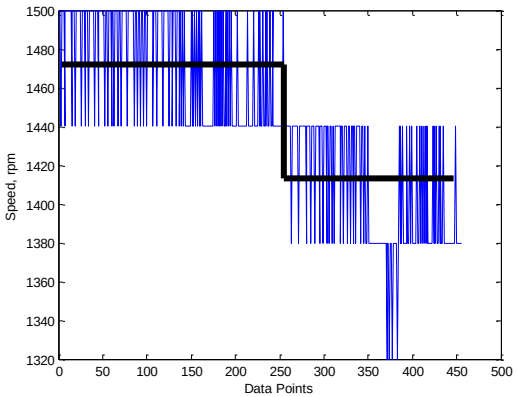

(f) When 20% of each Two Phases are short circuited through resistance R=3.1 ohm

Fig-20: Speed variation of TPIM under different loading conditions

IV. RESULTS AND DISCUSSION

Form the above results it is very clear that the TPIM under healthy conditions, 10%, 20%, 30% short circuited winding of one phase, 10% short circuited winding of each two phases, 20% short circuited winding of each two phases, and 10% short circuited winding of each three phases draw very different three phase currents for same loading conditions and produce very different toques.

The speed is reduced for same torque if one, two or three winding(s) are short circuited by 10%.

Similarly, the speed is reduced at faster rate for same torque if one or two winding(s) are short circuited by 20%.

Fig.20 portrays that speed reduction is less when one winding is short circuited by 10% as compared to same winding short circuited by 20%.

The results represents that the motor current increases differently when motor is healthy in comparison to the motor when one, two or three winding(s) short circuited by 10% and when one, or two winding(s) short circuited by 20%.

V. ON-LINE DATA ACQUISITION FROM EXPERIMENTAL SET UP OF TPIM

The above developed sensors and data acquisition system are interfaced with personal computer through the interfacing software developed in MS-Visual Studio. The acquired on-line data are shown in Fig. 21 and Fig. 22. This data is used for the estimation of stator and rotor parameters of TPIM. These on-line estimated parameters using GNA are plotted on the screen as shown in Fig. 22. The details of GNA parameter estimation is discussed in next section.

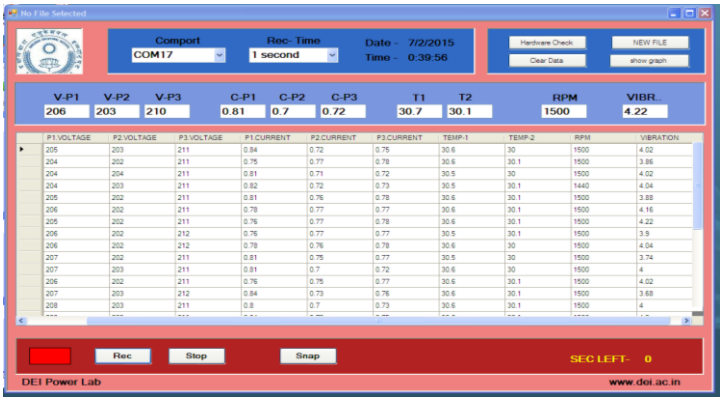

Fig.21 On-line data acquisition from experimental set up of TPIM

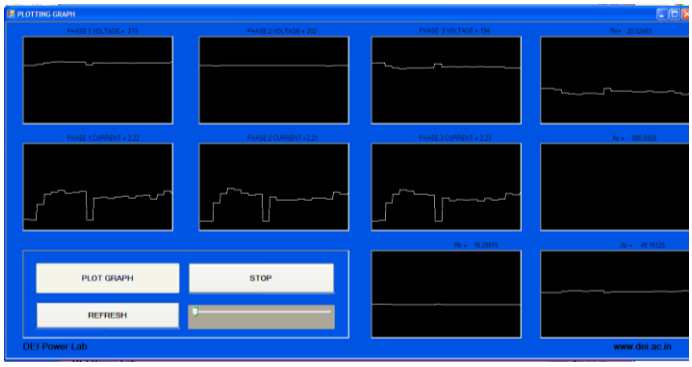

Fig. 22 On-line parameter estimation of TPIM using GNA

Parameter Estimation Using ANA and GNA

The above data is used as input for training of Artificial Neural Approach (ANA) and Generalized Neural Approach (GNA). These trained neural approaches are used for estimating the values of Ro, Xo, equivalent resistance and equivalent reactance. The ANA and GNA used for on line parameter estimation have following structure as given in Table 2.

Table -2: ANA and GNA structures

S.No.	Structure	ANA	GNA
	Inputs	2	2
	Outputs	4	4
	Hidden neurons	10	-
	Hidden layer Activation Function	***tanig***	***tansig and gaussian***
	layer Activation Function	Pure linear	Pure linear

The Levenberg-Marquet learning algorithm is used for training. The estimated parameters using ANA are illustrated in Table 3 at full load.

Table-3: Comparisons of Experimental and Estimated Values at full load

TPIM Parameters	Experimental Value(Ω)	Estimated Value by ANA (Ω)	% Error
R_o	21.18334	24.3	12.82%
X_o	195.3894	200.46	2.50%
R_b	23.01117	25.0112	8.01%
X_b	45.5996	48.59	5.4%

The TPIM parameters vary with TPIM temperature, applied frequency, ϕ-saturation, and operating point. The rotor network parameters are vital parameters for TPIM control. The rotor network resistances can changeup to 1.5 times over the whole operation.

The conventional ANA has some disadvantages such as learning rate, hidden layers of ANA and its connections, etc. To overcome some of its problems GNA is used in this work.

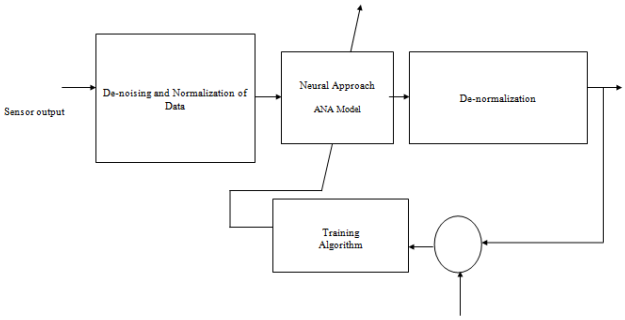

Fig-23: Block diagram of neural approach for parameter estimation

Table–4: Comparison of Experimental & Estimated Values using ANA and GNA we get the approximately same parameters

TPIM Parameters	Experimental Value(Ω)	Estimated Value by ANA (Ω)	Estimated Value by GNA (Ω)
Ro	21.1	24.3	22.1
Xo	195.38	200.46	198.49
Rb	23.011	25.0112	24.12
Xb	45.59	48.59	46.57

ON LINE PARAMETER ESTIMATION USING GNA

The voltage, current and power is acquired on-line and the TPIM parameters are estimated on-line using ANA and GNA. The results are tabulated in Table-4. The screen shot is also shown in Fig 22.

The speed- torque curve for these estimated parameters are compared with experimentally calculated parameters of healthy TPIM is shown in Fig. 24.

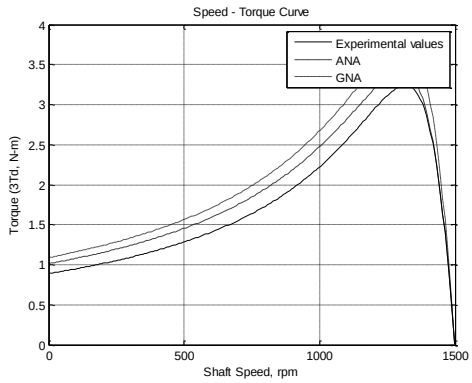

Fig-24: Comparison of speed – torque curves of TPIM for ANA, GNA and experimentally calculated parameters

Table-5: On Line Parameter Estimation under different loading conditions using ANA

	Loading condition					
	0%	25%	50%	75%	100%	150 %
Ro	19.55	20.05	21.07	22.7	24.3	24.5
Xo	182.4	185.8	190	196	200.5	209
Rb	22.61	22.78	22.88	22.9	25.01	23.9
Xb	44.84	45.22	46.62	47.8	48.59	50

Table-6: On Line Parameter Estimation under different loading conditions using GNA

	Loading condition					
	0%	25%	50%	75%	100%	150%
Ro	19.75	20.15	21.47	21.5	22.1	23.1
Xo	183.1	186.4	190.8	197	198.5	200
Rb	22.71	22.98	23.18	23.2	24.12	24.9
Xb	45.14	45.52	46.82	48.9	46.57	51

VI. CONCLUSION

This paper deals with the experimentation on TPIM under different motor conditions and also different loading conditions. It is found that the phase currents of TPIM are very different for different motor conditions and under different loading conditions. Similarly, the motor speed decreases at different rates. The information for motor currents, voltages and speed are used for on-line estimating the motor parameters (such as R_1, X_1, R_2, X_2 and shunt parameters (R_0 and X_0) of TPIM. The parameter estimation is done with neural approach such as ANA, GNA and compared with conventional methods.

The estimated parameters using proposed approaches have been used by the mathematical model of TPIM to plot the ω-T characteristics for validating the results.

It is found that the results obtained from GNA are better than other approaches

VII. REFERENCES

[1] Filippetti F., Franceschini G., Tassoni C., and Vas P., (2000), "Recent developments of induction motor drives fault diagnosis using AI techniques", IEEE Trans. Ind. Electron, vol. 47, no. 5, pp. 994–1004, Oct.

[2] Sulowicz M. and Sobczyk T. J., (2007), "Application of fuzzy inference system for cage induction motors rotor eccentricity diagnostic", Proc. IEEE Sdemped, pp. 101–105.

[3] Zidani F., Diallo D., Benbouzid M. E. H., and Nait-Said R., (2008), "A fuzzy based approach for the diagnosis of fault modes in a voltage-fed PWM inverter induction motor drives" ,IEEE Trans. Ind. Electron., vol. 55, no. 2, pp. 586–593.

[4] Balara D. and Timko J., (2000), "Identification of induction motor parameters with use of neural networks taking into account main flux saturation effect", Proc. 9th Int. Conf. EPE-PEMC. Ko¢ sice, Slovak Republic, pp. 6.17–6.23.

[5] Chow M. and Yee S. O., (1991), "Application of neural networks to incipient fault detection in induction motors", J. Neural Netw. Comput., vol. 2, no. 3, pp. 26–32.

[6] Demian C., Cirrincione G., and Capolino G. A., (2002), "A neural approach for fault diagnostics in induction machines", Proc. IEEE IECON, Sevilla, Spain, Nov.,vol. 4, pp. 3372–3376.

[7] Kowalski C. T. and Orlowska-Kowalska T., (2003), "Neural networks application for induction motor faults diagnosis", Math. Comput. Simul., vol. 63, no. 3–5, pp. 435–448, Nov.

[8] Yang B. S., Han T., and An J. L., (2004), "An ART-KOHONEN neural network for fault diagnosis of rotating machinery", Mech. Syst. Signal Process., vol. 18, no. 3, pp. 645–657, May.

[9] Chaturvedi D.K., "Soft Computing and Its Application in electrical Engineering", Springer – Verlag, Germany, 2008.

[10] Ayhan B., Chow M. Y., and Song M. H., (2006), "Multiple discriminate analysis and neural-network-based monolith and partition fault-detection schemes for broken rotor bar in induction motors", IEEE Trans. Ind. Electron., vol. 53, no. 4, pp. 1298–1308, Jun.

[11] Marcetic D.P. and Vukosavi´c S.N., (2007), "Speed-sensorless ac drives with the rotor time constant parameter update", IEEE Trans. Ind. Electron., vol. 54, no. 5, pp. 2618–2625, Oct.

[12] Su H. and Chong K. T., (2007), "Induction machine condition monitoring using neural network modeling", IEEE Trans. Ind. Electron., vol. 54, no. 1, pp. 241–249, Feb.
[13] Bouzid M. B. K., Champenois G., Bellaaj N. M., Signac L., and Jelassi K., (2008), "An effective neural approach for the automatic location of stator interturn faults in induction motor", IEEE Trans. Ind. Electron, vol. 55, no. 12, pp. 4277–4289, Dec.
[14] Chow T. W. S. and Hai S., (2004), "Induction machine fault diagnostic analysis with wavelet technique", IEEE Trans. Ind. Electron., vol. 51, no. 3, pp. 558–565, Jun.
[15] Cusido, L. Romeral, J. A. Ortega, J. A. Rosero, and A. Garcia Espinosa, (2008), "Fault detection in induction machines using power spectral density in wavelet decomposition", IEEE Trans. Ind. Electron., vol. 55, no. 2, pp. 633–643, Feb.
[16] Pons-Llinares J., Antonino-Daviu J. A., Riera-Guasp M., Pineda-Sanchez M., and Climente-Alarcon V., (2009), "Induction motor fault diagnosis based on analytic wavelet transform via frequency B-splines", Proc. IEEE SDEMPED, pp. 1–6.
[17] Mahamad A. K. and Hiyama T., (2009), "Improving Elman network using genetic algorithm for bearing failure diagnosis of induction motor", Proc. IEEE SDEMPED, pp. 1–6.
[18] Schiavo A Lo and Luciano A. M., (2001), "Powerful and Flexible Fuzzy Algorithm for Nonlinear Dynamic System Identification", IEEE Transactions on Fuzzy Systems, Vol. 9, No. 6.
[19] Koubaa Yassine , (2004), "Recursive identification of induction motor parameters", Simulation Modelling Practice and Theory 12 (2004) 363–381.
[20] Yamada T., Yabuta T., and Takahashi K., (1991), "Remarks on an adaptive type self-tuning controller using neural networks", IEEE IECON'91, pp. 1389-1394.
[21] Fukuda T. and Shibata T., (1992), "Theory and applications of neural networks for industrial control system", IEEE Trans. Ind. Electron., Vol. 39, pp. 472-489.
[22] Etxebarria V., (1994), "Adaptive control discrete systems using neural networks", IEE Roc.-Control Theory Appl., Vol. 141, No. 4, pp. 209-215,.
[23] Raison B., Francois F., Rostaing G., and Rogon J., (2000), "Induction drive speed monitoring by neural networks", Proc. IEEE Int. Conf. IECON, Nagoya, Japan, pp. 859–863.
[24] Silver Howard, (2006), "Neural Networks in Electrical Engineering",Proceedings of the ASEE New England Section 2006 Annual Conference, pp. 1-21.
[25] Narendra S. K. and Parthasarathy K., (1990), "Identification and control of dynamical systems using neural networks", IEEE Trans. Neural Networks, vol. 1, pp. 4–27, Jan.
[26] Ka´zmierkowski M. and Sobczuk D., (1994), "Investigation of neural network current regulator for VS-PWM inverters", Proc. Int. Conf. PEMC, Warsaw, Poland, vol. II, pp. 1009–1014..
[27] Ku C. C. and Lee KY K. Y., (1995), "Diagonal recurrent neural networks for dynamic systems control", IEEE Trans. Neural Networks, vol. 6, pp. 144–155, Jan.
[28] "Adaptive speed control for induction motor" motor drives using neural networks", IEEE Trans. Ind. Electron., vol. 42, no. 1, pp. 25–32, Feb.
[29] Simoes M. G. and Bose B. K., (1995), "Neural network based estimation of feedback signals for a vector controlled induction motor drive", IEEE Trans. Ind. Appl., vol. 31, no. 3, pp. 620–629, May/Jun.
[30] Narendra S. K., (1996), "Neural networks for control: Theory and practice", Proc. IEEE, vol. 84, pp. 1385–1406, Oct.
[31] Kulawski G. and Brdys H., (2000), "Stable adaptive control with recurrent networks", Automatica, vol. 36, no. 1, pp. 5–22, Jan.
[32] Chaturvedi DK & Malik OP (2005), A Generalized Neuron Based Adaptive Power System Stabilizer for Multimachine Environment, IEEE Trans. on Power Systems, Vol. 20, No. 1, Feb, pp.358-366.
[33] Chaturvedi DK & Malik OP (2008), Neuro-Fuzzy Power System Stabilizer, IEEE Trans. on Power Systems, Vol.23, No.3, Sept., pp. 887-894.

BIOGRAPHIES

D. K. Chaturvedi received the M.Tech. degree in Engineering Systems and management and the Ph.D. degree in electrical power systems from Dayalbagh Educational Institute (D.E.I.), Agra, India. He did Postdoctoral Research at the University of Calgary, Calgary AB, Canada. Currently, He is a Professor in the department of Electrical Engineering Faculty of Engineering at D.E.I.

Mayank Pratap Singh received the M.Tech. degree in Engineering Systems and the Ph.D. degree in electrical machines from Dayalbagh Educational Institute (D.E.I.), Agra, India. Currently, He is a Assistant Professor in the department of Electrical Engineering, GLA University, Mathura

O. P. Malik (M'66–SM'69–LF'00) received the Ph.D. degree from the University of London, London,. U.K., and the D.I.C. from the Imperial College, London, U.K., in 1965.Currently, he is a Emeritus Professor in the Department of Electrical and Computer Engineering at the University of Calgary, Calgary, AB, Canada, He has performed research work in collaboration with teams from Russia, Ukraine, China, and India. In addition to his research and teaching, he has served in many additional capacities at the University of Calgary including Associate Dean of Academics/Student Affairs and Acting Dean of the Faculty of Engineering.